Ind. J. Pharm. Edu. Res., 2023; 57(4):1029-1036.
https://www.ijper.org

Original Article

Identifying Potential Drug Candidates against *Plasmodium falciparum* (Isolate 3D7) through Targeting ADP-dependent DNA Helicase RecQ: An *in silico* Approach

Marya Ahsan[1,*], Ayaz Khurram Mallick[2]

[1]Department of Pharmacology, College of Medicine, Imam Mohammad Ibn Saud Islamic University (IMSIU), Riyadh, SAUDI ARABIA.
[2]Department of Clinical Biochemistry, College of Medicine, King Khalid University, Abha, SAUDI ARABIA.

ABSTRACT

Background: The malarial scenario has significantly varied in the past few decades; whether it is funding or the range of sophisticated life-saving tools that have been improved, the disease burden has reduced, and even a few nations are on the verge of their elimination. Despite these, drug resistance is the major hurdle in the fight against malaria. **Aim:** Identifying new drug candidates with negligible toxicity are imperative to overcome the existing problem. The proposed study aims to identify new potential lead molecules via targeting the ADP-dependent DNA helicase RecQ of *Plasmodium falciparum* (isolate 3D7) using Target-Based Virtual Screening (TBVS), molecular docking, and dynamics simulations. **Materials and Methods:** Ligand molecules were retrieved from a comprehensive digital library of the MCULE database having millions of investigational compounds. Pfizer's rule of five and the number of halogen atoms (3-5) were considered the basic primary filters of TBVS. The AutoDockVina (ADV) and GROningenMAchine for Chemical Simulations software were used to assess the molecular interactions and stability of protein-ligand complexes, respectively. **Results:** The primary filters of the TBVS work-pipeline depicted 2,597,040 chemical hits from over a hundred million small molecules. The toxicity tool sifted twenty-one molecules whose HIA and BBB permeation were evaluated through the Egan-Egg model. Five ligand hits were shortlisted with zero violation of drug-likeness and contain three or more hydrogen bonds. ADME, docking, and MD parameters depicted a molecule MCULE-1255186442-0-1 as a promising drug candidate. **Conclusion:** Druggable properties of identified ligands are inferred purely from the *in silico* experiments, so before its therapeutic implications, wet-lab validations are imperative.

Keywords: Malaria, *Plasmodium falciparum*, DNA helicase, PfWrn, Docking, MD simulation.

Correspondence:
Dr. Marya Ahsan
Department of Pharmacology, College of Medicine, Imam Mohammad Ibn Saud Islamic University (IMSIU), Riyadh-13317, SAUDI ARABIA.
Email: marya.ahsan@gmail.com

Received: 26-12-2022;
Revised: 22-02-2023;
Accepted: 31-05-2023.

INTRODUCTION

According to the World Malaria Report (WMR), The number of malaria cases worldwide has increased from 227 million to 241 million from 2019 to 2020. One of the deadliest and most pervasive parasitic diseases is malaria, brought on by the *Plasmodium* parasite and introduced to humans through the female *Anopheles* mosquito's bite.[1] The last line of defense against malaria is antimalarial medication. However, as the parasite and its mosquito vector are becoming increasingly resistant to insecticides and antimalarial medications currently on the market, it is getting harder to control the disease. Even the effectiveness of Artemisinin Combination Therapies (ACT) has decreased, leading to an increase in mortality worldwide. Five primary Plasmodium species cause malaria, including *Plasmodium knowlesi*, *Plasmodium vivax*, *Plasmodium ovale*, and *Plasmodium malariae*; the deadliest and most common is *P. falciparum*. India accounts for 3% of the global malaria burden, per the WMR 2019.[2,3] The ability to control the global disease burden is seriously threatened by the rapidly evolving drug-resistant strains against the new class of antimalarial drugs. There are three genomes in each species of Plasmodium: a nuclear genome, a mitochondrial genome, and an apicoplast genome. With 14 chromosomes, more than 7000 genes, and a four-stage life cycle involving humans, mosquitoes, and humans, the malaria parasite is large and complex.[4] The control of malaria is becoming more and more challenging due to the rapid spread of resistance of both the parasite and the mosquito vector to currently available antimalarial treatment modalities. RecQ protein family members play significant roles in DNA replication, transcription, repair, recombination, and telomere maintenance.[5-7] RecQ protein family members are a highly conserved group of DNA helicases. Humans have been found to

DOI: 10.5530/ijper.57.4.124

have five members of the RecQ family: RecQ1, RecQ2 (BLM), RecQ3 (WRN), RecQ4, and RecQ5, and only two RecQ family members are found in *P. falciparum*: PfWRN, which is encoded by the PF3D7 1429900 gene, and PfRecQ1 a.k.a. PfBLM, which is encoded by the PF3D7 0918600 gene.[6-8] Both proteins have 3′–5′ direction-specific DNA helicase activity and an ATPase. RecQ4 is human Werner homolog, akin to PfWrn in *P. falciparum*.[7-9] Recent studies suggest that PfRecQ1 and PfWRN contribute to DNA replication dynamics, gene expression patterns, and genome stability in *P. falciparum* (9). *P. falciparum* helicase PfBlm, which has a size of 85 kDa, is smaller than humans' HsBlm, which has a size of 159 kDa, while the size of *P. falciparum's* PfWRN (169 kDa) is slightly larger than the human (162 kDa) (4). PfBlm contains ATP-binding and helicase C-terminal domains of PfBlm protein,[8] but in PfWRN, the ATPase and DNA helicase activity present in the N-terminal domain (PfWrnN) of PfWrnN proteins. In addition, the involvement of more interacting proteins that the cell needs for a particular function is aided by this N and C-terminal extension.

It is also clear that the *P. falciparum* 3D7 strain's PfWrn protein is expressed throughout all stages of intraerythrocytic development and is primarily found in the nucleus.[4-10] Moreover, helicases interact with several other biological pathways that control autophagy, apoptosis, and homeostasis.[10-12] The PfWrn protein is present in the intraerythrocytic developmental stages of *P. falciparum*; therefore, targeting it can hinder the growth and transmission of the parasite in the human body.

3D structure of the ADP-dependent DNA helicase RecQ of *Plasmodium falciparum* (isolate 3D7) was retrieved from AlphaFoldDB due to the unavailability of its structure in PDB.[13] Evaluation of Alpha Fold's models is based on the protein Local Distance Difference Test (pLDDT) which predicts a confidence score between 0 and 100. To identify potential lead molecules, Structure-Based Virtual Screening (SBVS) with Lipinski rule of five (RO5: MW ≤ 500 Da; HBD ≤ 5; HBA ≤ 10; LogP ≤ 5) and halogen atoms (3-5) as the primary screening filtration was employed in MCULE's search workflow. The MCULE database contains millions of synthetic and purchasable molecules that could be used in cell-based bioassays and other experimental studies. Identified ligands were docked with DNA helicase via AutoDockVina (ADV) of the MCULE platform, and subsequently, a toxicity assessment was carried out. The Brain or IntestinaLEstimateD (BOILED)-Egg model of SwissADME was used to depict gastrointestinal absorption and brain penetration. Further, ligand hits were examined through other druggable features, and subsequent medicinal chemistry's Pan Assay Interference Structure (PAINS) and Brenk alert investigation were achieved. The top hits were carried out for Molecular Dynamics (MD) simulation.[14] A comparative analysis among various hits identified the best lead molecule.

MATERIALS AND METHODS

3D structure retrieval and preparation of protein

AlphaFoldDB was used for the 3D structure of the target protein ADP-dependent DNA helicase RecQ (UniProt ID: Q8ILG5) of *Plasmodium falciparum* (isolate 3D7).[15] AlphaFoldDB uses the Local Distance Difference Test (LDDT) to assess the qualities of their predicted models.[16] The energy minimization of selected protein was carried out through the CHARMm force field.[17,18]

Structure-based virtual screening

An online drug discovery platform MCULE was employed to identify diversified small molecules via SBVS. Five descriptors, like molecular weight (less than 500 g/mol), HBD (less than 5), HBA (less than10), lipophilicity (less than 5), and the number of halogen atoms (3-5) as initial search filters were used in the SBVS workflow. The threshold limit for homology and diversity was kept as 0.85 and 1000, respectively, in the input workflow. The FP2 fingerprint of open babel was assigned to screen investigational small molecules.[19,20]

Docking simulation

MCULE's ADV was utilized for molecular interaction studies between ADP-dependent DNA helicase RecQ and virtually-screened ligand hits. AutoDock Vina is one of the fastest and most widely used open source programs. It relies on robust and rigorous scoring functions as compared other docking programs. For docking analysis free energy of binding (ΔG) was considered as a standard parameter for the assessment of interaction potential. 3D structure of the protein was uploaded to the input workflow of the ADV interface. Grid size in x (-14.964 Å), y (-1.019 Å), and z (-1.0575 Å) axes were assigned to cover the binding pockets of protein. ADV parameters for binding mode per ligand and discretization were considered a default. The number of H-bonds and Free energy of binding (ΔG) was selected as the primary criterion for assessing the best conformation of selected hits that fitted into the binding pocket of the target protein.[21-24]

Toxicophores exclusion

Toxic moieties, fragments, scaffolds, and substructures that are desirable kinds of stuff in humans and ecosystems were identified through the "Toxicity Checker" tool inbuilt tools of the MCULE database. Toxicity Checker uses the simplified molecular-input line-entry system-based SMARTS algorithm.[19]

Evaluation of gastrointestinal absorption and blood-brain barrier permeation

The assessment of identified ligand hits was carried through the BOILED (Brain orIntestinaLEstimateD)-Egg model, which depicts Human Intestinal Absorption (HIA), and the Blood-Brain Barrier (BBB) permeation. Both BBB and HIA depend on two key physicochemical descriptors, including lipophilicity (WLOGP ≤

5.88) and topological polar surface area (TPSA ≤ 5.88 Å^2). The pictorial illustration of the model reveals how far a molecule is from the ideal one for ideal absorption.[25-28]

Assessment of medicinal chemistry attributes

Frequent hitters or promiscuous compounds were excluded by using two key medicinal chemistry attributes, viz., Pan Assay Interference Structure (PAINS) alert tool of the Eli Lilly biotech industry Moreover, mutagenic and carcinogenic substructures, dyes, and toxic moieties were kicked out through the Brenk's alert option of SwissADME.[29,30]

Stability assessment using MD simulation

At the Molecular Mechanics (MM) level, the top three protein-ligand docked complexes were simulated computationally at NTP using the open-source software package GROMACS 5.1.2 to evaluate their stabilities. The ligands were isolated from their individual protein complexes using the gmxgrep module. The topology and force field parameters were assigned through the CHARMm General Force Field (CGenFF) server. The topologies were created for ADP-dependent DNA helicase RecQ using pdb2gmx segments of the GROMACS package. The structural coordinates of the top three hits were achieved through the CGenFF tool.[31-33]

All protein-ligand complexes were saturated in a dodecahedron box of water molecules with a margin of 10 Å. The creation of boundary parameters of complexes was achieved via the gmxeditconf module. Neutralization of charges of protein-ligand complexes was carried through adding sodium and chloride ions, thereby preserving the biological concentration of 0.15 M. Subsequently, the system was energetically minimized for 2,50,000 steps using the robust steepest descent algorithm. The system temperature was maintained from 0-300K throughout their equilibration of 5ns duration at STP. After attaining equilibrium, the particle mesh was allotted via the Ewald scheme.[34,35] Various modules of the GROMACS package e.g., gmxrms, gmxrmsf, and gmxsasa, gmxΔGsolv, and gmxRg, were used to predict the stability of hits molecules in terms of RMSD, RMSF, SASA, ΔGsolv, and Rg attributes.[31-36]

RESULTS AND DISCUSSION

3D structure retrieval of ADP-dependent DNA helicase RecQ

The predicted 3D structure of the selected protein was extracted from AlphaFoldDB. It assesses the model through pLDDT, corresponding to the model's prediction of its score on the local Distance Difference Test (lDDT-Cα). It measures local accuracy for interpreting larger-scale features like relative domain positions. AlphaFold prediction relies on a per-residue confidence score derived from pLDDT ranges between 0 and 100.[13,15,16] The predicted model is shown in Figure 1.

Structure-based virtual screening and toxicity check

Upon applying the primary filtrations of Lipinski RO5 and the number of halogen atoms, the SBVS workflow estimated output count was found to be 25,970,40 ligand hits from more than a hundred million investigational ligand hits. Subsequent toxicity assessment was carried out through the toxicity checker of SwissADME. Dynamic and robust SMILES-based SMARTS algorithm exponentially narrowed the aforementioned data to only twenty-one chemical hits, excluding the toxicophoric moieties and scaffolds, and the remaining hits, 25,970,19, were rejected during rigorous toxicity evaluation.[25]

HIA and BBB permeation

Human intestinal absorption and blood-brain barrier permeation of toxicity-succeeded hits were evaluated through the BOILED-Egg model, a.k.a. Egan-Egg model relies on two key physiochemical properties viz., WLOGP and TPSA. White and yellow (yolk) regions show the ideal spaces for substantial HIA and brain penetration, respectively. Respectively, 15 and 6 molecules emerged as Pgp^+ and Pgp^-. Out of six Pgp^+ molecules, one ligand shows plausible BBB permeation, while the remaining are substantially GI-absorbable molecules. Moreover, out of fifteen Pgp^- compounds, respectively, two and eight are fairly brain penetrator and GI absorbable, while two molecules are on the white and yolk bord line, and two are neither HIA nor BBB permeable (Figure 2).[25,37]

Evaluation of druggable properties

To assess drug-likeness properties, identified hits were sifted through different bio-models, including Amgen's Ghose, GSK's Veber, Pharmacia's Egan, Bayer's Muegge rules, and Abbott's Bioavailability Score (BS).[27,28,38-41]These bio-models depict druggable properties of investigational hits intrinsically to develop upcoming possible oral drug compounds. Five ligand hits viz., MCULE-1255186442-0-1, MCULE-4030371218-0-1,MCULE-7384556744-0-1, MCULE-7861319803-0-64, and MCULE-4832832183-0-1 comply with the rules of three (out of five) bio-models were identified for further study. MCULE-1255186442-0-1andMCULE-4832832183-0-1exhibited one violation in Muegge (HBA>10) and Ghose (MW>480), respectively. Two molecules, viz., MCULE-4030371218-0-1 and MCULE-7384556744-0-1, obeyed all drug-likeness properties. While MCULE-7861319803-0-64 displayed two violations, one in Ghose (WLOGP>5.6) and another in Egan (WLOGP>5.88).

Molecular interaction analysis

Ligand hits succeeded through bio-models were carried out for their molecular docking into the binding pocket of ADP-dependent DNA helicase RecQ through exploiting the ADV tool to evaluate their binding propensity concerning free energy of binding (ΔG) that was in the range of -8.45 to -7.80 kcal/mol^{-1}. Among the top five hits, MCULE-1255186442-0-1

was the best as it exhibited minimum free energy of binding (ΔG: -8.45 kcal/mol), followed by MCULE-4030371218-0-1 (ΔG: -8.19 kcal/mol), MCULE-7384556744-0-1 (ΔG: -8.11 kcal/mol), MCULE-4832832183-0-1 (ΔG: -7.90 kcal/mol), and MCULE-7861319803-0-64 (ΔG: -7.80 kcal/mol). MCULE-1255186442-0-1 interacted with the binding crevice of protein with 17 residues via eight different binding interactions, viz., Vdw, HB, CHB, Alkyl, Pi-Cation, Pi-Alkyl, Pi-anion, and Halogen (Fluorine). (Figure 3A-B). Molecular interaction of MCULE-4030371218-0-1 and protein was stabilized through 16 residues via 8 different interacting forces viz., Vdw, HB, Alkyl, Pi-Alkyl, Pi-Donor HB, Pi-Sigma, Pi-Pi T-Shaped, and Halogen (Fluorine) (Figure 3C-D). MCULE-7384556744-0-1 interacted with 17 residues of protein through seven types of molecular forces e.g., Vdw, HB, Alkyl, Pi-Alkyl, Pi-Anion, Amide-Pi Stacked, and Halogen (Fluorine) (Figure 3E-F). Binding propensity and types of interaction involved in all top five ligand hits, the successor of drug-likeness filtration, is shown in Table 1.

Hydrogen bond analysis

MCULE-1255186442-0-1, MCULE-4030371218-0-1, and MCULE-7384556744-0-1 showed 4, 3, and 3 hydrogen bonds, respectively, during interaction with ADP-dependent DNA helicase RecQ. These three ligands showed a strong binding affinity with minimum ΔG values with ADP-dependent DNA helicase RecQ residues compared to other selected ligand hits. Therefore, only these ligands were taken forward for MD studies.[42-45]

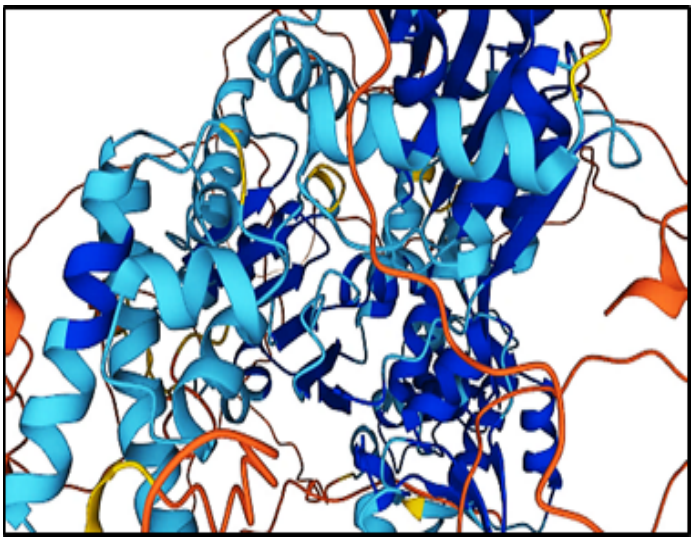

Figure 1: Predicted 3D model of ADP-dependent DNA helicase RecQ. Secondary Structure Elements (SSEs) highlight in blue exhibited very high confidence score (pLDDT> 90), SSEs in light blue depicts moderate confidence score Confident (90 >pLDDT> 70), Residues in yellow shows low confidence (70 >pLDDT> 50), while SSEs in orange exhibits very score Low (70 >pLDDT> 50).

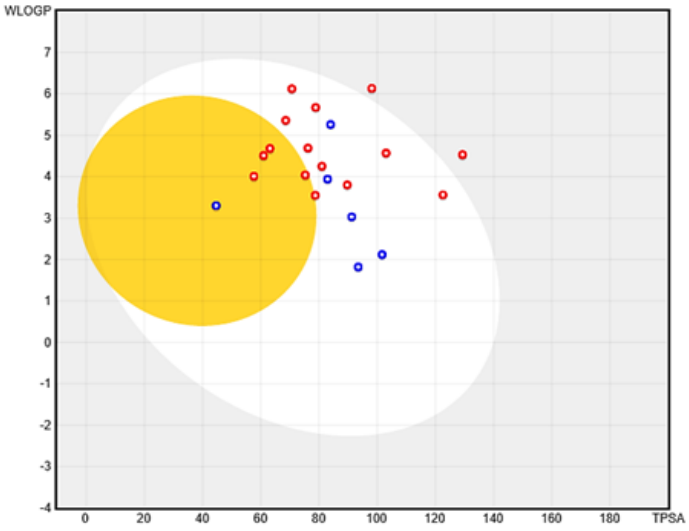

Figure 2: The BOILED-Egg (Egan-Egg model) evaluates the passive GI absorption and BBB permeation of toxicity succeeded ligands. Dots in the blue and red respectively exhibited substrate and non-substrate of P-glycoprotein.

Table 1: Binding affinity of the top five hits and type of interactions holding amino acid residues of ADP-dependent DNA helicase RecQ of *Plasmodium falciparum* (isolate 3D7).

Ligands	ADP-dependent DNA helicase RecQ	
	ΔG (kcal/mol^{-1})	Types of molecular interactions
MCULE-1255186442-0-1	-8.45	#Vdw, HB, CHB, Alkyl, Pi-Cation, Pi-Alkyl, Pi-anion and Halogen (Fluorine).
MCULE-4030371218-0-1	-8.19	Vdw, HB, Alkyl, Pi-Alkyl, Pi-Donor HB, Pi-Sigma, Pi-Pi T-Shaped, and Halogen (Fluorine).
MCULE-4832832183-0-1	-7.90	Vdw, HB, CHB, Alkyl, Pi-Cation, and Pi-Alkyl.
MCULE-7384556744-0-1	-8.11	Vdw, HB, Alkyl, Pi-Alkyl, Pi-Anion, Amide-Pi Stacked, and Halogen (Fluorine).
MCULE-7861319803-0-64	-7.80	Vdw, HB, Alkyl, Pi-Anion, Pi-Cation, Pi-Donor HB, and Halogen (Fluorine).

Vdw: Van der Waals, HB: Conventional Hydrogen Bond, CHB: Carbon Hydrogen Bond.

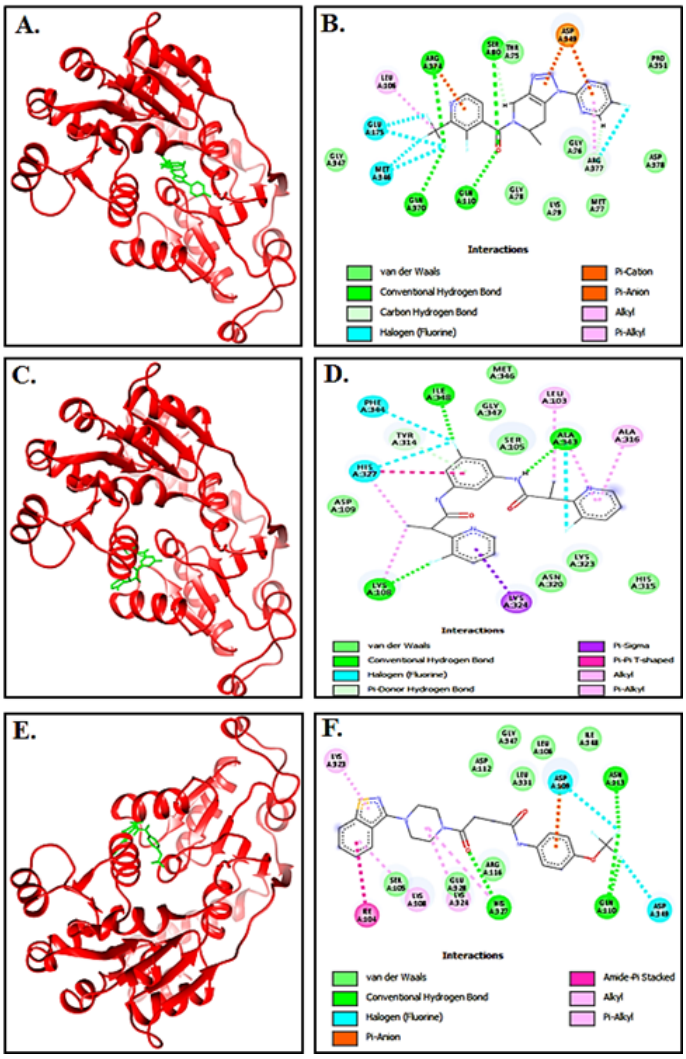

Figure 3: ADP-dependent DNA helicase RecQ -MCULE-1255186442-0-1 complex. (A) 3D pose of the MCULE-1255186442-0-1 complex (green stick) docked to the binding pocket of ADP-dependent DNA helicase RecQ. (B) 2D pose of MCULE-1255186442-0-1 binding with different residues of ADP-dependent DNA helicase RecQ. (C-D):ADP-dependent DNA helicase RecQ - MCULE-4030371218-0-1 complex. (C) 3D pose of the MCULE-4030371218-0-1 complex (green stick) docked to the binding pocket of ADP-dependent DNA helicase RecQ. (D) 2D pose of MCULE-4030371218-0-1 binding with different residues of ADP-dependent DNA helicase RecQ.(3 E-F):ADP-dependent DNA helicase RecQ - MCULE-7384556744-0-1 complex. (E) 3D pose of the MCULE-7384556744-0-1 complex (green stick) docked to the binding pocket of ADP-dependent DNA helicase RecQ. (F) 2D pose of MCULE-7384556744-0-1binding with different residues of ADP-dependent DNA helicase RecQ.

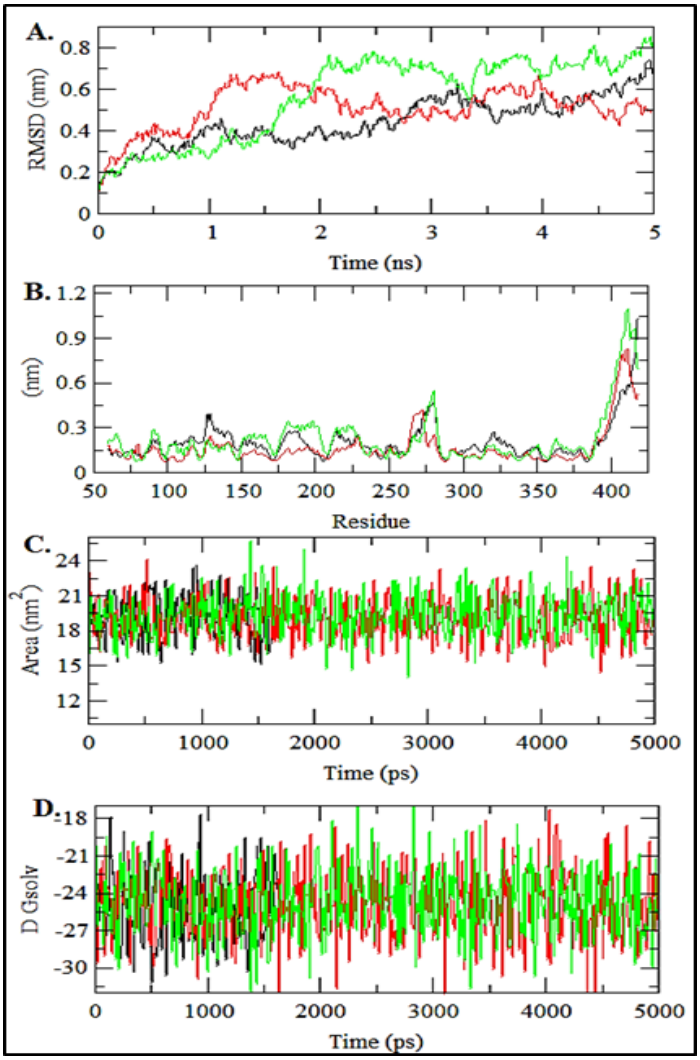

Figure 4: (A) RMSD plot as a function of time. Black, red, and green represent values computed. for ADP-dependent DNA helicase RecQ-MCULE-1255186442-0-1, MCULE-4030371218-0-1, and MCULE-7384556744-0-1, respectively. (B) RMSF plot for ADP-dependent DNA helicase RecQ –MCULE-1255186442-0-1 (black), MCULE-4030371218-0-1 (red), and MCULE-7384556744-0-1 (green). (C) SASA plot for ADP-dependent DNA helicase RecQ-MCULE-1255186442-0-1 (black), MCULE-4030371218-0-1 (red), and MCULE-7384556744-0-1 (green). (D) ΔGsolv plot for ADP-dependent DNA helicase RecQ-MCULE-1255186442-0-1 (black), MCULE-4030371218-0-1 (red), and MCULE-7384556744-0-1 (green).

Stability evaluation of docked complexes

The stability of docked complexes of the top three ligand hits viz., MCULE-1255186442-0-1, MCULE-4030371218-0-1, and MCULE-7384556744-0-1 with ADP-dependent DNA helicase RecQ was inspected through MD simulations of 5 ns duration at Dell Workstation Precision 3440 using GROMACS package. MD graphs for RMSD, RMSF, SASA, ΔGsolv, Rg, and HBs were plotted to evaluate the molecular docking stability of ligands and protein-docked complexes.[31]

Root-mean-square deviation

The RMSD elucidates the stability of docked complexes.[46-48] The average RMSD for MCULE-1255186442-0-1 (black), MCULE-4030371218-0-1 (red), and MCULE-7384556744-0-1 (green) with ADP-dependent DNA helicase RecQ was found 0.44 nm, 0.51, and 0.57 nm, respectively. The RMSD plot reveals that the stability of docked complex of protein and MCULE-1255186442-0-1 is the least as compared to the remaining two (Figure 4A).

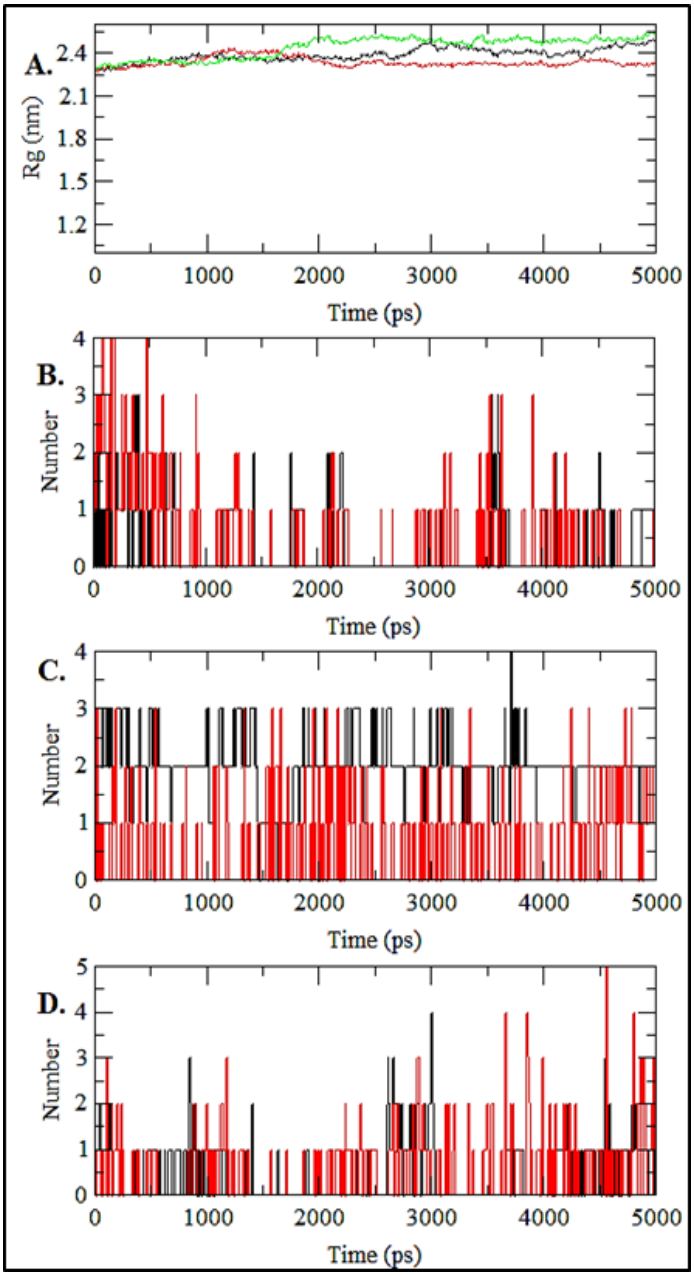

Figure 5: (A) Rg plot for ADP-dependent DNA helicase RecQ-MCULE-1255186442-0-1 (black), MCULE-4030371218-0-1 (red), and MCULE-7384556744-0-1 (green).Hydrogen bond analysis. (B) HB plot shows the formation and deformation of H-bonds during interaction of ADP-dependent DNA helicase RecQ with MCULE-1255186442-0-1, (C) MCULE-4030371218-0-1, (D) MCULE-7384556744-0-1.

Root-mean-square fluctuation

The residues fluctuations at various positions of the RMSF plot are due to the binding interactions of ligand hits, MCULE-1255186442-0-1 (black), MCULE-4030371218-0-1 (red), and MCULE-7384556744-0-1 (green) withADP-dependent DNA helicase RecQ. Average residues fluctuation upon binding with ligands was found to be 0.20 nm, 0.17 nm, and 0.22 nm, respectively (Figure 4B).

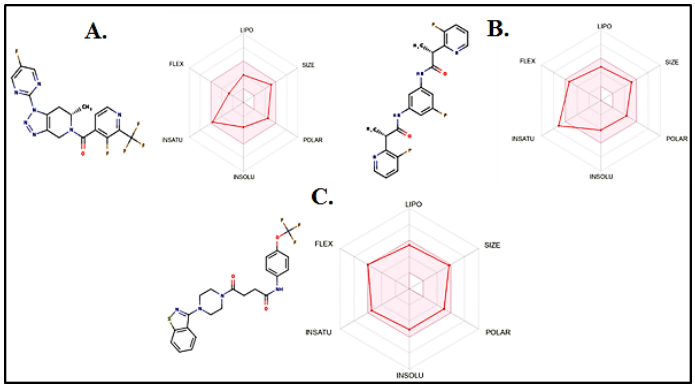

Figure 6: The bioavailability radar for A) MCULE-1255186442, B) MCULE-4030371218-0-1, and C) MCULE-7384556744-0-1. The bioavailability radar is based on Lipophilicity (LIPO), Size (MW), Polarity (POLAR), Insolubility (INSOLU), Instauration (INSATU), and Flexibility (FLEX) to depict pro-drug attributes.

Solvent-accessible surface area

The surface area of the protein, which is covered by the solvent molecule, isillustrated by the SASA graph.[49,50] The mean value of SASA upon binding with MCULE-1255186442-0-1 (black), MCULE-4030371218-0-1 (red), and MCULE-7384556744-0-1 (green) was found as 19.28 nm^2, 19.14 nm^2, and 19.38 nm^2, respectively (Figure 4C).

Free energy of solvation

The average ΔGsolv of ADP-dependent DNA helicase RecQ upon binding with MCULE-1255186442-0-1 (black), MCULE-4030371218-0-1 (red), and MCULE-7384556744-0-1 (green)was depicted as -24.97 kJ/mol/nm^2, -24.77 kJ/mol/nm^2, and -24.68 kJ/mol/nm^2, respectively (Figure 4D).

Radius of gyration

The compactness of protein-ligand complexes is measured by the radius of the gyration plot,which is inversely proportional to the compactness. The average Rg values of docked complexes of MCULE-1255186442-0-1 (black), MCULE-4030371218-0-1 (red), and MCULE-7384556744-0-1 (green) were computed as 2.39 nm, 2.34 nm, and 2.44 nm, respectively (Figure 5A).

Hydrogen bond formations, deformation, and stability of selected protein-ligand complexes during MD studies are illustrated in hydrogen plots. Four hydrogen bonds were formed during the docking of ADP-dependent DNA helicase RecQ and MCULE-1255186442-0-1,they did not attain stability for the entire simulation process (Figure 5B). Three HB were formed in ADP-dependent DNA helicase RecQ -MCULE-4030371218-0-1, but one HBwas found stable (Figure 5C), while in the case of MCULE-7384556744-0-1, 5 HBs were depicted,but only one HB attained stability till the whole process (Figure 5D).

Moreover, the bioavailability radar based on Lipophilicity (LIPO), Size (MW), Polarity (POLAR), Insolubility (INSOLU),

Instauration (INSATU), and Flexibility (FLEX) to depict pro-drug attributes[25] is shown in Figure 6. The radar illustrates that selected ligand hits are ideally located in the hexagonal (pink) area, except for the unsaturation of MCULE-4030371218-0-1. Even though MCULE-4030371218-0-1 comply with Lipinski's RO5, it is inferred that these ligand hits are appropriate for oral leads. MCULE-1255186442, compared to others, could be promising as it suited all parameters adopted in the study. Albeit having substantial druggable properties, wet-lab validations of insilico findings are desirable before exploring their therapeutic implications against malaria.

CONCLUSION

ADP-dependent DNA helicase RecQ of *Plasmodium falciparum* (isolate 3D7) is a putative molecular target that could be therapeutically promising for antimalarial therapy. High-throughput SBVS, toxicity profiling, physicochemical properties, lipophilicity, solubility, pharmacokinetics, drug-likeness, medicinal chemistry attributes, molecular docking, RMSD, RMSF, SASA, ΔGsolv, Rg, and HBs analyses establish that MCULE-1255186442 encompasses all druggable features that are essentially pertained to oral drug molecules. Molecular interactions are the fundamental part of all organisms ensuing in an excellent coordinated way and associated with virtually all their cellular functions. Molecular interaction forms the basis of molecular recognition. The molecular and cellular processes within living systems proceed in an equilibrium between necessities to remain and what ought to decline. All organisms relentlessly shed cells that have received signals to pass on, which is essential if tissues are reproduced or stay young and healthy. Stability of predicted molecules was assessed on various druggable parameters. Thus, in the horizon of the insilico predictions, MCULE-1255186442 may have developed as a substantial oral drug candidate against *Plasmodium falciparum* (isolate 3D7). However, experimental studies are required before using its therapeutic inferences.

ACKNOWLEDGEMENT

The author thanks Almanac Life Science India Pvt. Ltd., for important contributions to the work.

CONFLICT OF INTEREST

The authors declare no conflict of interest.

ABBREVIATIONS

WMR: World Malaria Report; **ACT:** Artemisinin Combination Therapies; **SBVS:** Structure-Based Virtual Screening; **ADV:** Auto Dock Vina; **TPSA:** Topological Polar Surface Area; **MM:** Molecular Mechanics; **BS:** Bioavailability Score.

REFERENCES

1. Akinosoglou KS, Solomou EE, Gogos CA. Malaria: A haematological disease. Hematology. 2012;17(2):106-14. doi: 10.1179/102453312X13221316477336, PMID 22664049.
2. Tuteja R. Malaria – an overview. FEBS Journal. 2007;274(18):4670-9. doi: 10.1111/j.1742-4658.2007.05997.x, PMID 17824953.
3. Cowman AF, Healer J, Marapana D, Marsh K. Malaria: biology and disease. Cell. 2016;167(3):610-24. doi: 10.1016/j.cell.2016.07.055, PMID 27768886.
4. Rahman F, Tarique M, Ahmad M, Tuteja R. *Plasmodium falciparum* Werner homologue is a nuclear protein and its biochemical activities reside in the N-terminal region. Protoplasma. 2016;253(1):45-60. doi: 10.1007/s00709-015-0785-6, PMID 25824666.
5. Roach ES, Anselm I, Rosman NP, Caplan LR. Progeria. Uncommon Causes Stroke. 2008:2nd ed.
6. Khakhar RR, Cobb JA, Bjergbaek L, Hickson ID, Gasser SM. RecQ helicases: multipleroles in genome maintenance. Trends Cell Biol. 2003;13(9):493-501. doi: 10.1016/s0962-8924(03)00171-5, PMID 12946629.
7. Claessens A, Harris LM, Stanojcic S, Chappell L, Stanton A, Kuk N, *et al*. RecQ helicases in the malaria parasite *Plasmodium falciparum* affect genome stability, gene expression patterns and DNA replication dynamics. PLOS Genet. 2018;14(7):e1007490. doi: 10.1371/journal.pgen.1007490, PMID 29965959.
8. Tuteja R. Genome wide identification of *Plasmodium falciparum* helicases: A comparison with human host. Cell Cycle. 2010;9(1):104-20. doi: 10.4161/cc.9.1.10241, PMID 20016272.
9. Rahman F, Tarique M, Tuteja R. *Plasmodium falciparum* Bloomhomologue, a nucleocytoplasmic protein, translocates in 3′ to 5′ direction and is essential for parasite growth. Biochim Biophys Acta. 2016;1864(5):594-608. doi: 10.1016/j.bbapap.2016.02.016, PMID 26917473.
10. Shih JW, Lee YH. Human DExD/H RNA helicases: emerging roles in stress survival regulation. Clin Chim Acta. 2014;436:45-58. doi: 10.1016/j.cca.2014.05.003, PMID 24835919.
11. Hu G, McQuiston T, Bernard A, Park YD, Qiu J, Vural A, *et al*. A conservedmechanism of TOR-dependent RCK-mediated MRNA degradation regulates autophagy. Nat Cell Biol. 2015;17(7):930-42. doi: 10.1038/ncb3189, PMID 26098573.
12. Szczesny RJ, Obriot H, Paczkowska A, Jedrzejczak R, Dmochowska A, Bartnik E, *et al*. Down-regulation of Human RNA/DNA helicase SUV3 induces apoptosis by a caspase- and AIF-dependent pathway. Biol Cell. 2007;99(6):323-32. doi: 10.1042/BC20060108, PMID 17352692.
13. Jumper J, Evans R, Pritzel A, Green T, Figurnov M, Ronneberger O, *et al*. Highly accurate protein structure prediction with alpha Fold. Nature. 2021;596(7873):583-9. doi: 10.1038/s41586-021-03819-2, PMID 34265844.
14. Alwabli AS. Lead identification against 3C-like protease of SARS-CoV-2 Via Target-based Virtual Screening and Molecular Dynamics simulation. J Young Pharm. 2022;14(2):179-86. doi: 10.5530/jyp.2022.14.34.
15. Varadi M, Anyango S, Deshpande M, Nair S, Natassia C, Yordanova G, *et al*. Alpha Fold protein structure database: massively expanding the structural coverage of protein-sequence space with high-accuracy models. Nucleic Acids Res. 2022;50(D1):D439-44. doi: 10.1093/nar/gkab1061, PMID 34791371.
16. Mariani V, Biasini M, Barbato A, Schwede T. lDD T: a local superposition-free score for comparing protein structures and models using distance difference tests. Bioinformatics. 2013;29(21):2722-8. doi: 10.1093/bioinformatics/btt473, PMID 23986568.
17. Brooks BR, Bruccoleri RE, Olafson BD, States DJ, Swaminathan S, Karplus M. CHARMM: A program for macromolecular energy, minimization, and dynamics calculations. J Comput Chem. 1983;4(2):187-217. doi: 10.1002/jcc.540040211.
18. Ahmad KMK, Salman A, Al-Khodairy SF, Al-Marshad F M, Abdulrahman AM, Arif Jamal M. Computational Exploration of dibenzo [a,l] pyrene Interaction to DNA and Its Bases: possible Implications to Human Health. Biointerface Res Appl Chem. 2020;11(4):11272-83. doi: 10.33263/BRIAC114.1127211283.
19. Hanwell MD, Curtis DE, Lonie DC, Vandermeersch T, Zurek E, Hutchison GR. Avogadro: an advanced semantic chemical editor, visualization, and analysis platform. J Cheminform. 2012;4(1):17. doi: 10.1186/1758-2946-4-17, PMID 22889332.
20. Shakil S. Molecular interaction of investigationalligands with human brain acetylcholinesterase. J Cell Biochem. 2019;120(7):11820-30. doi: 10.1002/jcb.28461, PMID 30746750.
21. Steffen C, Thomas K, Huniar U, Hellweg A, Rubner O, Schroer A. TmoleX–a graphical user interface for TURBOMOLE. J Comput Chem. 2010;31(16):2967-70. doi: 10.1002/jcc.21576, PMID 20928852.
22. Ajijur R, Salman A, Ahmad KMK. Combinatorial design to deciphernovellead molecule against *Mycobacterium tuberculosis*. Biointerface Res Appl Chem. 2021;11(5):12993-3004. doi: 10.33263/BRIAC115.1299313004.
23. Khan MKA, Akhtar S, Arif JM. Development of *in silico* protocols to predict structural insights into the metabolic activation pathways of xenobiotics. Interdiscip Sci. 2018;10(2):329-45. doi: 10.1007/s12539-017-0237-4, PMID 28527150.
24. Khan MKA, Akhtar S, Arif JM. Structural insight into the mechanism of dibenzo [a,l]pyrene and benzo [a] pyrene-mediated cell proliferation using molecular docking simulations. Interdiscip Sci. 2018;10(4):653-73. doi: 10.1007/s12539-017-0226-7, PMID 28374118.

25. Daina A, Michielin O, Zoete V. Swiss ADME: A freewebtool to evaluate pharmacokinetics, drug-likeness and medicinal chemistry friendliness of small molecules. Sci Rep. 2017;7:42717. doi: 10.1038/srep42717, PMID 28256516.
26. Attique SA, Hassan M, Usman M, Atif RM, Mahboob S, Al-Ghanim KA, *et al*. A molecular docking approach to evaluate the pharmacological properties of natural and synthetic treatment candidates for use against hypertension. Int J Environ Res Public Health. 2019;16(6):923. doi: 10.3390/ijerph16060923, PMID 30875817.
27. Egan WJ, Merz KM, Baldwin JJ. Prediction of drug absorption using multivariate statistics. J Med Chem. 2000;43(21):3867-77. doi: 10.1021/jm000292e, PMID 11052792.
28. Egan WJ, Lauri G. Prediction of intestinal permeability. Adv Drug Deliv Rev. 2002;54(3):273-89. doi: 10.1016/S0169-409X(02)00004-2, PMID 11922948.
29. Baell JB, Holloway GA. New substructure filters for removal of Panassay Interference Compounds (PAINS) from screening libraries and for their exclusion in bioassays. J Med Chem. 2010;53(7):2719-40. doi: 10.1021/jm901137j, PMID 20131845.
30. Brenk R, Schipani A, James D, Krasowski A, Gilbert IH, Frearson J, *et al*. Lessons learnt from assembling screening libraries for drug discovery for neglected diseases. ChemMedChem. 2008;3(3):435-44. doi: 10.1002/cmdc.200700139, PMID 18064617.
31. van der Spoel D, Lindahl E, Hess B, Groenhof G, Mark AE, Berendsen HJC. GROMACS: fast, flexible, and free. J Comput Chem. 2005;26(16):1701-18. doi: 10.1002/jcc.20291, PMID 16211538.
32. Vanommeslaeghe K, MacKerell AD. Automation of the CHARMM General Force Field (CGenFF) I: Bond perception and atom typing. J Chem Inf Model. 2012;52(12):3144-54. doi: 10.1021/ci300363c, PMID 23146088.
33. Vanommeslaeghe K, Hatcher E, Acharya C, Kundu S, Zhong S, Shim J, *et al*. CHARMM general force field: A force field for drug-like molecules compatible with the CHARMMall- atom additive biological force fields. J Comput Chem. 2010;31(4):671-90. doi: 10.1002/jcc.21367, PMID 19575467.
34. Petersen HG. Accuracy and efficiency of the particle meshEwald method. J Chem Phys. 1995;103(9):3668-79. doi: 10.1063/1.470043.
35. Stenberg S, Stenqvist B. An exact Ewald summation method in theory and practice. J Phys Chem A. 2020;124(19):3943-6. doi: 10.1021/acs.jpca.0c01684, PMID 32285671.
36. Fischer NM, van Maaren PJ, Ditz JC, Yildirim A, van der Spoel D. Properties of organic liquids when simulated with long-range Lennard-Jones interactions. J Chem Theor Comput. 2015;11(7):2938-44. doi: 10.1021/acs.jctc.5b00190, PMID 26575731.
37. Khan MKA, Ahmad S, Rabbani G, Shahab U, Khan MS. Target-based virtual screening, computational multiscoring docking and Molecular Dynamics simulation of small molecules as promising drug candidate affecting kinesin-like protein KIFC1. Cell Biochem Funct. 2022;40(5):451-72. doi: 10.1002/cbf.3707, PMID 35758564.
38. Ghose AK, Viswanadhan VN, Wendoloski JJ. A knowledge-based approach in designing combinatorial or medicinal chemistry libraries for drug discovery. 1. A qualitative and quantitative characterization of known drug databases. J Comb Chem. 1999;1(1):55-68. doi: 10.1021/cc9800071, PMID 10746014.
39. Veber DF, Johnson SR, Cheng HY, Smith BR, Ward KW, Kopple KD. Molecular properties that influence the oral bioavailability of drug candidates. J Med Chem. 2002;45(12):2615-23. doi: 10.1021/jm020017n, PMID 12036371.
40. Muegge I, Heald SL, Brittelli D. Simple selection criteria for drug-like chemical matter. J Med Chem. 2001;44(12):1841-6. doi: 10.1021/jm015507e, PMID 11384230.
41. Martin YC. A bioavailablity score. J Med Chem. 2005;48(9):3164-70. doi: 10.1021/jm0492002, PMID 15857122.
42. Kausar MA, Shahid S, Anwar S, Kuddus M, Khan MKA, Alotaibi AD, *et al*. Identifying natural therapeutics against diabetes via inhibition of dipeptidyl peptidase 4: molecular docking and MD simulation study. Indian J Pharm Educ Res. 2022;56(1s):s21-31. doi: 10.5530/ijper.56.1s.39.
43. Kausar MA, Shahid S, Anwar S, Kuddus M, Khan MKA, Khalifa AM, *et al*. Identifying the alpha-glucosidase inhibitory potential of dietaryphytochemicals against diabetes mellitusType 2 via molecular interactions and dynamics simulation. Cell Mol Biol (Noisy-Le-Grand). 2022;67(5):16-26. doi: 10.14715/cmb/2021.67.5.3, PMID 35818276.
44. Arwansyah A, Arif AR, Syahputra G, Sukarti S, Kurniawan I. Theoretical studies of thiazolyl-pyrazoline derivatives as promising drugs against malaria by QSAR modelling combined with molecular docking and molecular dynamics simulation. Mol Simul. 2021;47(12):988-1001. doi: 10.1080/08927022.2021.1935926.
45. Nguyen PTV, Nguyen GLT, Thi Đinh O, Duong CQ, Nguyen LH, Truong TN. In search of suitable protein targets for antimalarial and anti-dengue drug discovery. J Mol Struct. 2022;1256:132520. doi: 10.1016/j.molstruc.2022.132520.
46. Khurana J, Shrivastava A, Singh A, Gupta A. Exploring potential of Plasmodium RUVBL proteins as antimalarial drug target. J Biomol Struct Dyn. 2023;41(2):736-52. doi: 10.1080/07391102.2021.2011418, PMID 34877896.
47. Wong KKV, Roney M, Uddin N, Imran S, Gazali AM, Zamri N, *et al*. Usnic acid as potential inhibitors of BCL2 and P13K protein through network pharmacology-based analysis, molecular docking and molecular dynamic simulation. J Biomol Struct Dyn. 2023;1-14. doi: 10.1080/07391102.2023.2178506.
48. Al-Shuaeeb RAA, Yassin AA, Ibrahim MAA, Abd El-Mageed HR, Ghandour MA, Khalil MM. Computer-based identification of olive oil components as a potential inhibitor of neirisaral adhesion a regulatory protein. J Biomol Struct Dyn. 2023;41(5):1553-60. doi: 10.1080/07391102.2021.2022535, PMID 34974817.
49. Khoshbin Z, Housaindokht MR. Computer-Aided aptamer design for sulfadimethoxine antibiotic: step by step mutation based on MD simulation approach. J Biomol Struct Dyn. 2020;39(9):1-9.
50. Hollingsworth SA, Dror RO. Molecular Dynamics simulation for all. Neuron. 2018;99(6):1129-43. doi: 10.1016/j.neuron.2018.08.011, PMID 30236283.

Cite this article: Ahsan M, Mallick AK. Identifying Potential Drug Candidates against *Plasmodium falciparum* (Isolate 3D7) through Targeting ADP-dependent DNA Helicase RecQ: An *in silico* Approach. Indian J of Pharmaceutical Education and Research. 2023;57(4):1029-36.